Journal of Wind Engineering & Industrial Aerodynamics 177 (2018) 60–68

Contents lists available at ScienceDirect

Journal of Wind Engineering & Industrial Aerodynamics

journal homepage: www.elsevier.com/locate/jweia

A numerical study of the aerodynamic characteristics of ice-accreted transmission lines

Takeshi Ishihara [a,*], Shinichi Oka [b]

[a] Department of Civil Engineering, School of Engineering, The University of Tokyo, 7-3-1 Hongo, Bunkyo-ku, Tokyo 113-8656, Japan
[b] NUMECA Japan Co., Ltd., Kitamura Bldg., 1-17-15, Nishi-shinbashi, Minato-ku, Tokyo 105-0003, Japan

ARTICLE INFO

Keywords:
LES
Aerodynamic coefficients
Ice heights effect
Wake effect
Correction coefficient

ABSTRACT

Aerodynamic coefficients of single and 4-bundled ice-accreted conductors are investigated using the LES turbulence model and compared with the results of the wind tunnel test. Single conductors with span lengths of $L = 1D$ and $10D$ are simulated, and the predicted aerodynamic coefficients with a span length of $L = 10D$ show good agreement with the measured those within the estimated error range of the wind tunnel test, where D is the diameter of the single conductor. A systematic error estimation using the models with $L = 2D$, $3D$, and $6D$ is conducted; the results show that a span length of $L = 10D$ is long enough to predict aerodynamic coefficients. The effect of the accreted ice height, H, on the aerodynamic coefficients is investigated. It is found that negative pressure at the lower face near the leading edge significantly affects C_L and C_M and leads to the maximum absolute values of C_L and C_M at 12° for the conductor with $H = 1D$ and at 16° for the conductor with $H = 0.5D$. The wake effect of 4-bundled conductors is also investigated by the analysis of the aerodynamic coefficients and the pressure distribution for each conductor. The wake of the windward conductors has a significant impact on C_L and C_M. Correction coefficients for leeward conductors are proposed to account for the wake effect, and the results show good agreement with the predicted aerodynamic coefficients of the 4-bundled conductors.

1. Introduction

Large-amplitude wind-induced vibrations of ice-accreted transmission lines, called galloping, a form of single-degree-of-freedom aerodynamic instability, which can occur for long bodies with certain cross-sections (Holmes, 2001), could cause inter-phase short circuits or damage to insulators and support structures; in the worst case, such damage results in the shutdown of a transmission line (Scanlan, 1972). Hence, it is important to understand and evaluate the galloping phenomenon to establish countermeasures to prevent an accident. Many studies have reported the assessment of the galloping phenomenon (Den Hartog, 1956; Parkinson, 1971; Novak, 1972; Cooper, 1973; Kimura et al., 1999; Matsumiya and Nishihara, 2012). In a galloping evaluation, numerical analysis based on a quasi-steady approach is widely used in which the aerodynamic coefficients are obtained first and then response analysis is performed to evaluate the amplitude of vibrations. Software has been developed to predict the response of a transmission line. For example, Shimizu and Sato (2001) developed a finite element analysis code that accounts for the geometrical non-linearity of a transmission line, by which galloping simulations and analysis of the vibration characteristics are conducted. In general, aerodynamic coefficients are required for input data in such code. It is possible to obtain aerodynamic coefficients of ice-accreted transmission lines using a wind tunnel test (Shimizu et al., 2004; Matsumiya et al., 2010). However, a wind tunnel test is time consuming and costly because of the need to create a new model every time for each test. The aerodynamic coefficients of each sub-conductor must be obtained to predict the galloping of 4-bundled conductors accurately (Matsumiya and Nishihara, 2013). Shimizu et al. (2004) proposed a method to convert the aerodynamic coefficients of a single conductor into those of 4-bundled conductors; the results were in good agreement with those for the 4-bundled conductor by the wind tunnel test with regard to C_D and C_L, but a discrepancy was observed in C_M because the wake effect was not taken into account in the method. Matsumiya et al. (2010) clarified the wake effects of windward conductors on the leeward conductors using pressure measurements for all of the sub-conductors. However, in contrast to the force balance test, it is difficult to create models with pressure measurement probes. In addition, the locations and the number of measurement points are sensitive to the results.

Recently, numerical analysis has become a popular method for

* Corresponding author.
E-mail address: ishihara@bridge.t.u-tokyo.ac.jp (T. Ishihara).

https://doi.org/10.1016/j.jweia.2018.04.008
Received 28 August 2017; Received in revised form 25 November 2017; Accepted 9 April 2018
Available online 24 April 2018

obtaining aerodynamic coefficients of bluff bodies, such as circular cylinders and rectangular prisms. Oka and Ishihara (2009) used LES to predict the aerodynamic coefficients of a square prism, and they were found to be in good agreement with the wind tunnel test results. In addition, Oka and Ishihara (2010) showed that the aerodynamic coefficients of a single conductor using LES for ice-accreted transmissions lines were in good agreement with the experiments for the region of angle of attacks from 0° to 12°. However, a discrepancy was found between 16° and 20°, where the lift coefficients change substantially. In that research, correction formulas were proposed for the 4-bundled conductor model, for which the wake effects of windward conductors were taken into account, and improvements were observed in predicting C_D at angles of attack in the range from 0° to 90°; however, no results were presented for C_L or C_M.

Based on the above discussion, a numerical analysis of single-conductor transmission lines is conducted to clarify the impact of the span length on the accuracy of the aerodynamic coefficients. Firstly, the span length independent aerodynamic coefficients are evaluated to determine a span length that is sufficiently long to capture the three-dimensionality of turbulence. Next, the aerodynamic coefficients with respect to the different height of the accreted ice are investigated and effects of the height of the accreted ice on the aerodynamic characteristics are clarified by the predicted pressure distributions. Finally, the aerodynamic coefficients and pressure distributions of sub-conductors for 4-bundled conductors are investigated to show the wake effects of windward conductors on the aerodynamic coefficients of leeward conductors. In addition, correction coefficients are proposed for leeward conductors in the conversion from the single-conductor aerodynamic coefficients to the 4-bundled conductor ones to account for the wake effect.

2. Numerical model and boundary conditions

2.1. Governing equations

The governing equations for the LES model are obtained by filtering the time-dependent Navier-Stokes equations as follows:

$$\frac{\partial \rho \tilde{u}_i}{\partial x_i} = 0, \tag{1}$$

$$\frac{\partial}{\partial t}(\rho \tilde{u}_i) + \frac{\partial}{\partial x_j}(\rho \tilde{u}_i \tilde{u}_j) = \frac{\partial}{\partial x_j}\left(\mu \frac{\partial \tilde{u}_i}{\partial x_j}\right) - \frac{\partial \tilde{P}}{\partial x_i} - \frac{\partial \tau_{ij}}{\partial x_j}, \tag{2}$$

where $\tilde{u}_j$ and $\tilde{p}$ are the filtered mean velocity and the filtered pressure, respectively. ρ is the density, and τ_{ij} is the subgrid-scale stress defined by

$$\tau_{ij} = \rho \tilde{u}_i \tilde{u}_j - \rho \widetilde{u_i u_j} \tag{3}$$

The subgrid-scale stresses resulting from the filtering operations are unknown and are modeled as follows:

$$\tau_{ij} = -2\mu_t \tilde{S}_{ij} + \frac{1}{3}\tau_{kk}\delta_{ij}, \tag{4}$$

where μ_t is the subgrid-scale turbulent viscosity and $\tilde{S}_{ij}$ is the rate-of-strain tensor for the resolved scale and is defined by

$$\tilde{S}_{ij} = \frac{1}{2}\left(\frac{\partial \tilde{u}_i}{\partial x_j} + \frac{\partial \tilde{u}_j}{\partial x_i}\right). \tag{5}$$

The Smagorinsky model (Smagorinsky, 1963) is used for the subgrid-scale turbulent viscosity, μ_t.

$$\mu_t = \rho L_s^2 |\tilde{S}| = \rho L_s \sqrt{2\tilde{S}_{ij}\tilde{S}_{ij}}, \tag{6}$$

where L_s is the mixing length for subgrid-scales and is defined as

$$L_s = \min(\kappa\delta, C_s V^{1/3}). \tag{7}$$

where κ is the von Karman constant, 0.42; C_s is the Smagorinsky constant, with 0.032 used in this study (Oka and Ishihara, 2009); δ is the distance to the closest wall; and V is the volume of a computational cell.

2.2. Boundary conditions

When a wall-adjacent cell is in the laminar sublayer, the wall shear stress is obtained from the laminar stress-strain relationship as follows:

$$\frac{\tilde{u}}{u_\tau} = \frac{\rho u_\tau y}{\mu}, \tag{8}$$

If a mesh cannot resolve the laminar sublayer, then it is assumed that the centroid of the wall-adjacent cells falls within the logarithmic region of the boundary layer, and the law-of-the-wall is employed.

$$\frac{\tilde{u}}{u\tau_\tau} = \frac{1}{\kappa}\ln E\left(\frac{\rho u_\tau y}{\mu}\right). \tag{9}$$

where $\tilde{u}$ is the filtered velocity that is tangential to the wall, u_τ is the friction velocity, κ is the von Kármán constant, and the constant E has a value of 9.8. The uniform velocity condition is specified at the inlet boundary, and the zero-diffusive conditions are used at the outlet boundary. Symmetry conditions are given for both sides and for the upper/lower boundaries.

2.3. Numerical set-up

The finite volume method and the unstructured collocated mesh are used for the present simulations. The second-order central difference scheme is used for the convective and viscosity term, and the second-order implicit scheme is used for the unsteady term. The SIMPLE (Semi-Implicit Pressure Linked Equations) algorithm is employed for solving the discretized equations (Ferziger and Peric, 2002). All simulations are performed with ANSYS FLUENT.

Fig. 1 shows the cross-sectional dimensions of the ice-accreted conductor geometry models used in this study. Table 1 shows the major parameters for the analysis. Fig. 2 shows the mesh near the ice-accreted single conductor in which the diameter of the single

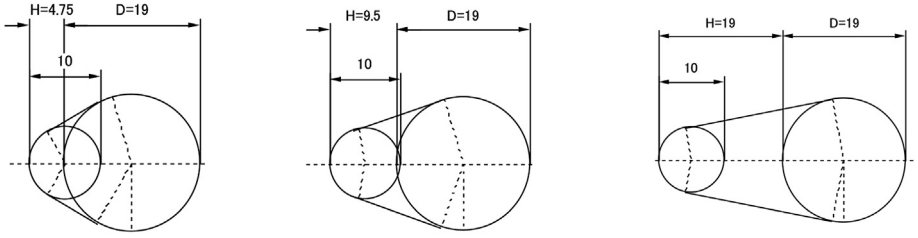

(a)) H=0.25D (b) H=0.5D (c) H=1D

Fig. 1. Cross-sectional dimensions of the conductors and the accreted ice geometry.